In vivo photoacoustic (PA) mapping of sentinel lymph nodes (SLNs) using carbon nanotubes (CNTs) as a contrast agent

Manojit Pramanik, Kwang Hyun Song, Magdalena Swierczewska, Danielle Green, Balaji Sitharaman, et al.

Manojit Pramanik, Kwang Hyun Song, Magdalena Swierczewska, Danielle Green, Balaji Sitharaman, Lihong V. Wang, "In vivo photoacoustic (PA) mapping of sentinel lymph nodes (SLNs) using carbon nanotubes (CNTs) as a contrast agent," Proc. SPIE 7177, Photons Plus Ultrasound: Imaging and Sensing 2009, 71771N (24 February 2009); doi: 10.1117/12.808522

SPIE.

Event: SPIE BiOS, 2009, San Jose, California, United States

In vivo photoacoustic (PA) mapping of sentinel lymph nodes (SLNs) using carbon nanotubes (CNTs) as a contrast agent

Manojit Pramanik[1], Kwang Hyun Song[1], Magdalena Swierczewska[2], Danielle Green[2], Balaji Sitharaman[2*], and Lihong V. Wang[1†]
[1]Optical Imaging Laboratory, Department of Biomedical Engineering, Washington University in St. Louis, St. Louis, MO, USA 63130;
[2]Department of Biomedical Engineering, State University of New York at Stony Brook, Stony Brook, New York, USA 11794

ABSTRACT

Sentinel lymph node biopsy (SLNB), a less invasive alternative to axillary lymph node dissection (ALND), is routinely used in clinic for staging breast cancer. In SLNB, lymphatic mapping with radio-labeled sulfur colloid and/or blue dye helps identify the sentinel lymph node (SLN), which is most likely to contain metastatic breast cancer. Even though SLNB, using both methylene blue and radioactive tracers, has a high identification rate, it still relies on an invasive surgical procedure, with associated morbidity. In this study, we have demonstrated a non-invasive single-walled carbon nanotube (SWNT)-enhanced photoacoustic (PA) identification of SLN in a rat model. We have used single-walled carbon nanotubes (SWNTs) as a photoacoustic contrast agent to map non-invasively the sentinel lymph nodes (SLNs) in a rat model *in vivo*. We were able to identify the SLN non-invasively with high contrast to noise ratio (~90) and high resolution (~500 μm). Due to the broad photoacoustic spectrum of these nanotubes in the near infrared wavelength window we could easily choose a suitable light wavelength to maximize the imaging depth. Our results suggest that this technology could be a useful clinical tool, allowing clinicians to identify SLNs non-invasively *in vivo*. In the future, these contrast agents could be functionalized to do molecular photoacoustic imaging.

Keywords: Sentinel lymph node biopsy, axillary lymph node dissection, breast cancer, photoacoustic tomography, carbon nanotube, single-walled carbon nanotube

1. INTRODUCTION

For the majority of invasive breast cancers, the surgical removal of primary breast tumor and level I and level II axillary lymph node dissections (ALND) are widely performed.[1] However, the common side effects after ALND include upper-extremity lymphedema, arm numbness, impaired shoulder mobility, arm weakness, and infections in the breast, chest, or arm.[2] A less invasive, more accurate alternative to axillary lymph node dissection (ALND) is sentinel lymph node biopsy (SLNB). For patients with clinically node-negative breast cancer, SLNB has rapidly become the standard of care.[3,4] Although this approach avoids ALND – associated morbidity, its safety depends on the accuracy of the sentinel lymph node (SLN) biopsy. In SLNB, a SLN is identified using lymphatic mapping with radio-labeled sulfur colloid and/or blue dye. A SLN is most likely to contain metastatic breast cancer. Thus, the pathologic status of the axilla can be predicted once the SLN is identified. There are a number of practical limitations to SLNB, particularly an identification rate and sensitivity of this technique are less than 95%, even in experienced hands.[3-5] Moreover, the complications of SLNB procedure include seroma formation, lymphedema, sensory nerve injury, and limitation in range of motion.[6] These limitations of SLNB strongly suggest that alternative strategies to stage the axilla should be explored.

Axillary ultrasound (AUS) is a potentially valuable technique for identifying axillary metastases.[7-9] AUS can visualize the lymph node is size, shape, and contour, as well as changes in cortical morphology and texture that appear to be

* Email: balaji.sitharaman@stonybrook.edu (nanotubes)
† Email: lhwang@biomed.wsutl.edu (photoacoustics)

Photons Plus Ultrasound: Imaging and Sensing 2009, edited by Alexander A. Oraevsky, Lihong V. Wang,
Proc. of SPIE Vol. 7177, 71771N · © 2009 SPIE · CCC code: 1605-7422/09/$18 · doi: 10.1117/12.808522

associated with the presence of axillary metastases. However, the ability of AUS alone to stage the axilla accurately is limited because of the sonographic signs of metastatic disease may overlap with those of benign reactive changes. Therefore, *in vivo* identification of a SLN would allow non-invasive axillary staging, with either percutaneous fine needle aspiration biopsy (FNAB) or other emerging molecular techniques.

Scientists and clinicians acquire *in vivo* images of anatomy and physiology of whole animals and humans with the help of numerous noninvasive imaging modalities, such as computed tomography (CT), single photon emission computed tomography (SPECT), positron emission tomography (PET), magnetic resonance imaging (MRI), ultrasound imaging (US), radio frequency (rf), and optical imaging. Strengths and weaknesses of each of these *in vivo* imaging techniques make them suitable for different applications. For each imaging modality, contrast agents have been developed not only to improve the contrast of the acquired images but also for molecular imaging by targeting specific biomolecules, cell tracking, and gene expression. In the last decade, much attention has been given to development of imaging techniques based on photoacoustic tomography (PAT) because of high spatial resolution and high soft tissue contrast.[10-12] Consequently, contrast agents have also been developed for PAT. Recently, carbon nanotube (CNT)-based contrast agents has shown promise for a variety of imaging techniques. Here, we have exploited the intrinsic optical absorbance of carbon nanotubes towards their development as contrast agents for photoacoustic (PA) imaging of the SLN. CNTs were first accumulated in the SLN in a rat model, and then PA images were taken to identify the SLN. The results of this research suggest that this PA technique may provide an alternative method to localize a SLN accurately.

2. METHODS AND MATERIALS

A reflection-mode PA imaging system[13] was used to get the PA spectroscopy of the single-walled carbon nanotubes (SWNTs). A tunable Ti:sapphire laser (LT-2211A, LOTIS TII) or a tunable dye laser (ND6000, Continuum) pumped by Q-switched Nd:YAG (LS-2137, LOTIS II) laser was the light source, which provided <15 ns pulse duration and a 10-Hz pulse repetition rate. Dark-field ring-shaped illumination was used in the system. The light energy on the sample surface was controlled to conform to the ANSI standard of maximum permissible exposure (MPE).[14] A 5 MHz central frequency, spherically focused (2.54 cm focus length, 1.91 cm diameter active area element and 72% bandwidth) ultrasonic transducer (V308, Panametrics-NDT) was used to acquire the generated PA signals. The signal was then amplified by a low-noise amplifier (5072PR, Panametrics-NDT), and recorded using a digital oscilloscope (TDS 5054, Tektronix) with a 50 mega-sampling rate. PA signal fluctuations due to pulse-to-pulse energy variation were compensated by signals from a photodiode (DET110, Thorlabs), which sampled the energy of each laser pulse.

2.1 Photoacoustic Imaging

A linear translation stage (XY-6060, Danaher Motion) was used for raster scanning to obtain three-dimensional (3-D) PA data. A computer controlled the stage and synchronized it with the data acquisition. To shorten the data acquisition time, a continuous scan was used without signal averaging. An A-line (A-scan) was the PA signal obtained along the depth direction at a single point. Multiple A-lines (acquired by a one-dimensional (1-D) scan) gave a two-dimensional (2-D) B-scan. A 3-D image was acquired with a 2-D scan. A 1-D depth-resolved image was obtained by multiplying the time axis of the initial A-scan (resolved in time along the depth direction) by the speed of sound in soft tissue (~1500 m/s).

The scanning time depends on the laser pulse repetition rate (PRR), the scanning step size, and the field of view (FOV). Typical values are a scanning step size for a 1-D scan = 0.1 mm, for a 2-D scan = 0.2 mm, a laser PRR = 10 Hz, and a FOV = 20 mm × 20 mm. The acquisition time = ~25 sec for a B-scan, and = ~42 min for a 3-D image. The transducer was located inside a water container with an opening of 5 cm x 5 cm at the bottom, sealed with a thin, clear membrane. The object was placed under the membrane, and ultrasonic gel was used for coupling the sound.

2.2 Animal and Drug Information

Guidelines on the care and the use of laboratory animals at Washington University in St. Louis were followed for all animal experiments. Adult Sprague Dawley rats with various body weights (250 - 350 g) were used for experiments.

Initial anesthetization of the rat was done using a mixture of ketamine (85 mg/kg) and xylazine (15 mg/kg). The hair on the region of interest of the rat was gently removed before imaging, using a commercial hair-removal lotion. Intradermal injection of 0.075 ml of 0.5 mg/ml SWNTs was performed on a left/right forepaw pad, depending on which side was imaged. Photoacoustic images were acquired after the administration of SWNTs. During the data acquisition, anesthesia was maintained using vaporized isoflurane (1 L/min oxygen and 0.75% isoflurane, Euthanex Corp.), and a pulse oximeter (NONIN Medical INC., 8600V) was used to monitor the vitals. If needed, 8 ml of 0.9% saline was administered to the rat for hydration. After image acquisition, the animal was euthanized by pentobarbital overdose.

2.3 Single-walled carbon nanotubes (SWNTs) synthesis

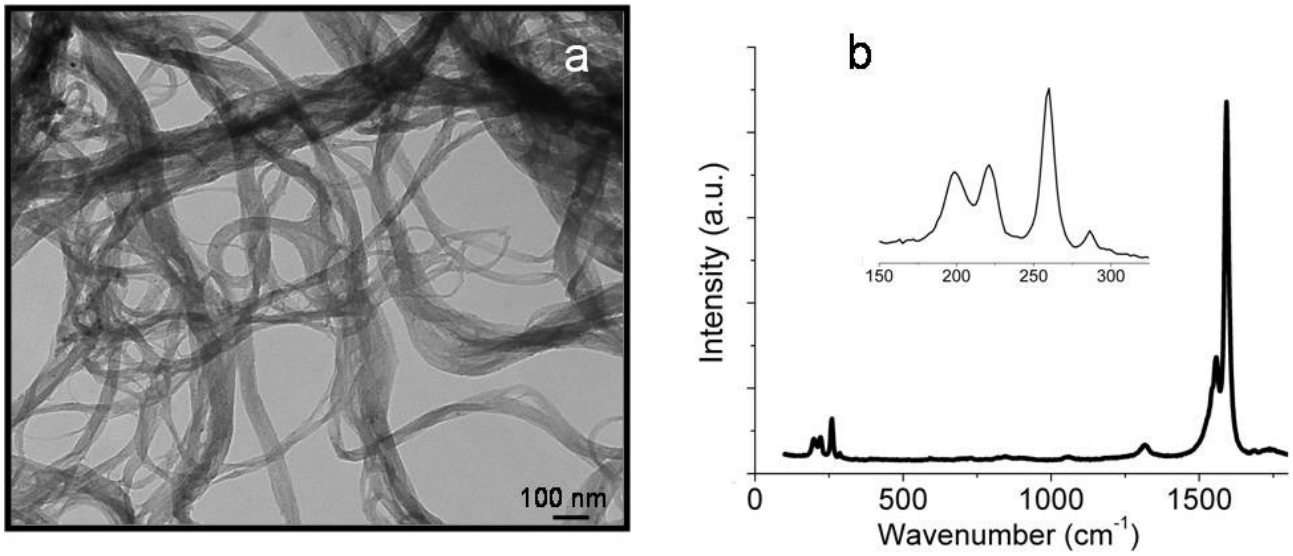

Figure 1. (a) TEM image of the SWNTs. (b) Complete Raman spectra showing D-band and G-band of the SWNTs. The inset shows the radial breathing modes.

Chemical vapor deposition was used to synthesize the carbon nanotubes via Fe catalysts. Fe nanoparticles were coated onto a silicon wafer using a diblock copolymer templating method.[17] These coated wafers were placed into a 3 inch quartz reaction chamber (Easy Tube 2000, First Nano). The chamber was first heated up to 900°C in Ar and filled with H_2 for 2 minutes. To initiate the growth of SWNTs, CH4 was added to the gas flow for 20 minutes. Lastly, the carbon feedstock was switched off and the furnace was cooled to room temperature. Raman spectroscopy (LabRAM Aramis, Horiba JvonYvon) at 633 nm excitation and transmission electron microscope (TEM) imaging (FEI Tecnai12 BioTwinG2) at 80 kV were used to characterize the SWNTs. Figures 1(a) and 1(b) show the low-resolution bright field TEM and Raman spectrum, respectively. The Raman spectrum shows a G band at 1592 cm^{-1} and a D band at 1315 cm^{-1}. The G band is a peak specific to graphene, while the D band indicates defects on the graphene sheet. The low D band to G band ratio signifies few defects in the SWNT sample. The radial breathing modes, which occur in the presence of small diameter tubes of graphene, can be viewed within the inset, and further confirm that these samples are SWNTs.

3. RESULTS AND DISCUSSIONS

3.1 Photoacoustic spectroscopy of SWNTs

Figure 2(a) shows the PA signals obtained from a tube (Silastic® laboratory tubing, Dow Corning Corp., with I.D. 300 μm, O.D. 640 μm) filled with SWNTs (0.5 mg/ml) and rat blood. 736 nm wavelength laser was the light source. Figure 2(b) shows the PA spectrum (peak-to-peak PA signal amplitude versus excitation light wavelength) of the SWNTs (in black) for an excitation wavelength range of 736-795 nm. The PA spectrum of rat blood (in red dotted line) is also shown in the same figure. It is evident that the PA signal obtained from SWNTs is stronger than the PA signal obtained from rat blood over the entire wavelength range. Therefore we can choose a specific light wavelength for imaging within a broad range. Due to the weak blood absorption, the NIR window is well known for providing deep tissue PA imaging at the expense of blood contrast. The strong PA signal from SWNTs in the NIR region implies that they could be used as contrast agents to boost the signal strength for PA imaging in this region.

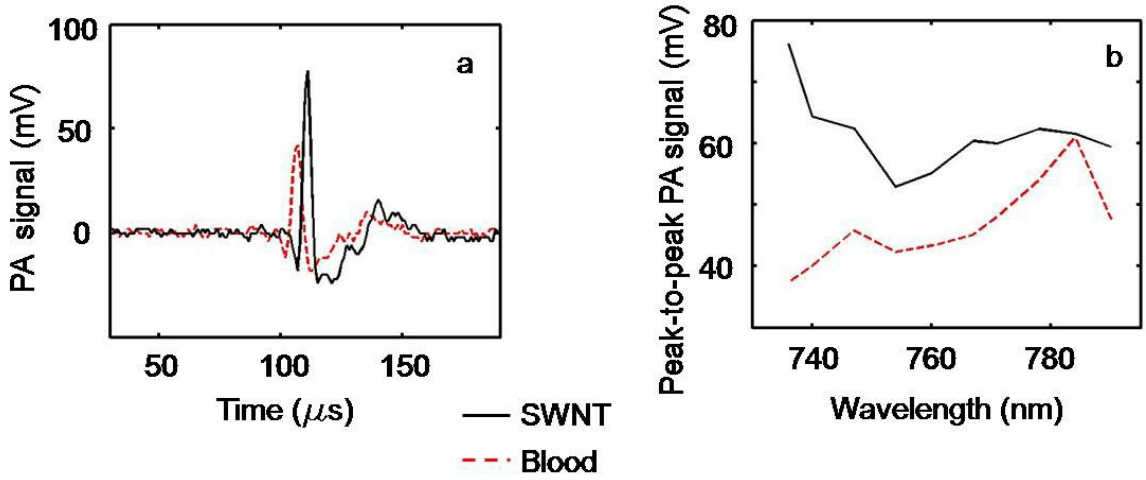

Figure 2. (a) Photoacoustic signals generated from a tube (Silastic® laboratory tubing, Dow Corning Corp., with I.D. 300 μm, O.D. 640 μm) filled with SWNTs (0.5 mg/ml) and rat blood. The excitation light was of 736 nm wavelength. (b) Photoacoustic spectrum of SWNTs and blood over a 736-795 nm wavelength range.

3.2 *In vitro* signal from SWNTs mixed with blood

In vitro tests were carried out with SWNTs mixed with blood at different proportion and then PA signals were recorded. The light used was of 767 nm wavelength. A tube (Silastic® laboratory tubing, Dow Corning Corp., with I.D. 300 μm, O.D. 640 μm) filled with blood, blood (90% v/v) + SWNTs (10% v/v), blood (75% v/v) + SWNTs (25% v/v), blood (50% v/v) + SWNTs (50% v/v), blood (25% v/v) + SWNTs (75% v/v), and SWNTs alone. Figure 3 shows the peak-to-peak PA signal amplitudes for those six samples, clearly indicating that the PA signal from blood enhanced when SWNTs were mixed with the blood. When 75% SWNTs were mixed with 25% blood we recorded the strongest PA signal, 1.14 V compared to signal from pure blood 0.45 V. Thus, we saw a more than 150% increase in the PA signal from blood when SWNTs were mixed with the blood.

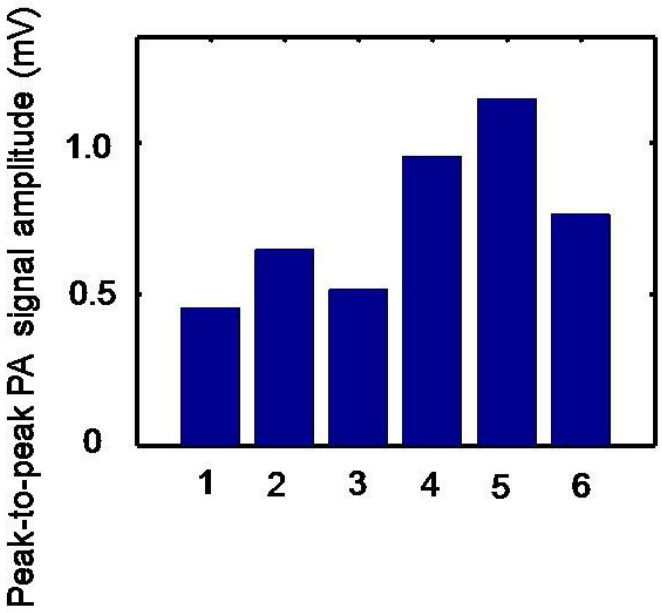

Figure 3. Peak-to-peak photoacoustic signal amplitudes for various blood sample. 1. Blood, 2. Blood (90% v/v) + SWNTs (10% v/v), 3. Blood (75% v/v) + SWNTs (25% v/v), 4. Blood (50% v/v) + SWNTs (50% v/v), 5. Blood (25% v/v) + SWNTs (75% v/v), and 6. SWNTs only. The excitation light was of 767 nm wavelength.

3.3 Sentinel Lymph Node imaging in a Rat *In vivo*

A rat SLN was clearly imaged by non-invasive *in vivo* PA imaging. Figure 4(a) is a representative photograph of a rat taken prior to image acquisition with the hair removed from axillary surface. Before SWNTs injection, a PA control image was obtained, which is shown in the form of a maximum amplitude projection (Figure 4(b)).[18] The vasculature near an axial node (one blood vessel is marked with BV) was clearly imaged. Figure 4(c) shows the PA image (MAP) of the same area immediately after the SWNTs were injected. Figure 4(d) is the post-injection PA images (MAP) of the same area after 190 min. The SLN is marked with a red dotted circle in figure 4(b). The signal amplitude of the surrounding blood vessels was also increased since some of SWNTs flowed into the blood stream and the nearby tissue. Figure 4(e) is a photograph of the same rat with the skin removed after PA imaging was done. Figure 4(f) is a photograph of the SLN removed from the rat. Figures 4(g) and 3(h) show the B-scan image corresponding to figures 4(b) and 4(d), respectively. The strong PA signal from the SLN is clear seen in figure 4(h), marked with red arrow. We used a 0.5 mg/ml concentration of SWNTs for our *in vivo* study (the average molecular weight of SWNTs is ~10^6 Da or g/mol; 0.5 mg/ml = 0.5 mg/ml/10^6 g/ml = 500 nM). However, that choice does not limit the use of SWNTs at other lower concentrations.[20] Our system is capable of detecting SWNTs on the order of nM concentration.

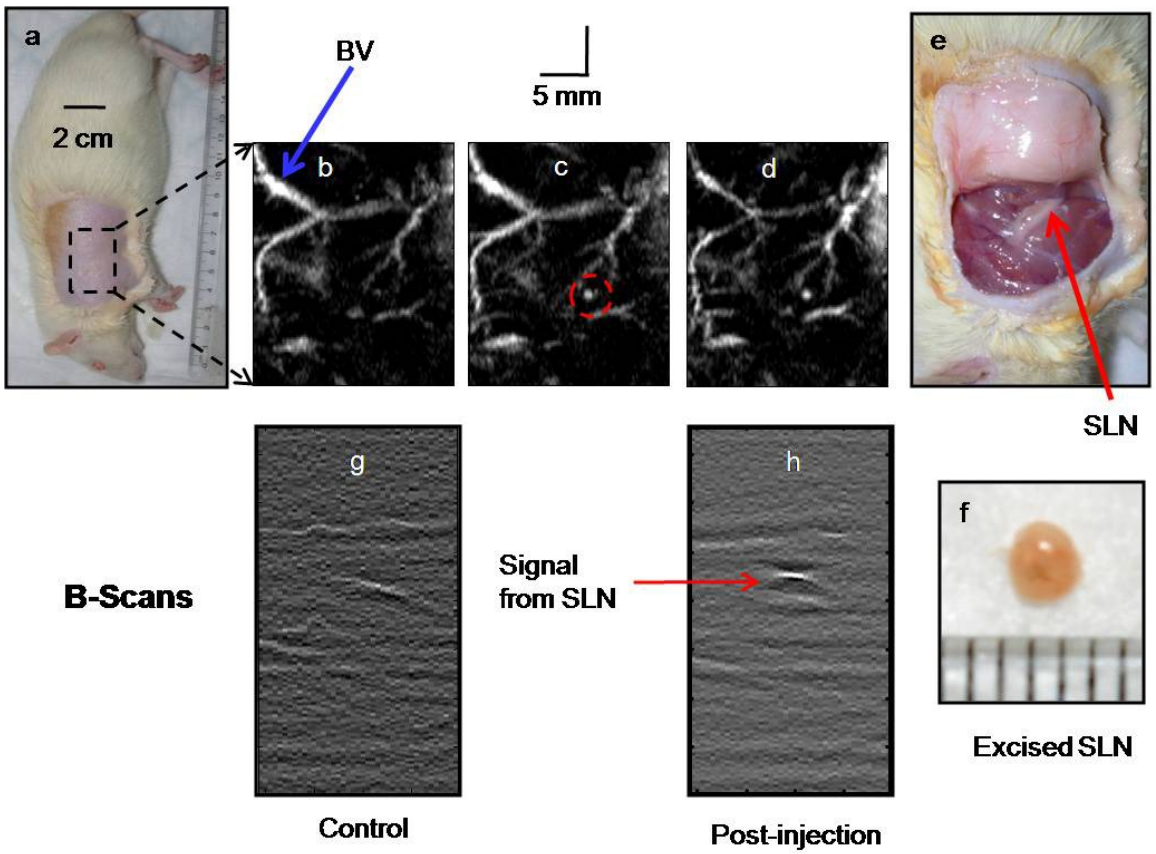

Figure 4. Non-invasive *in vivo* photoacoustic MAP images of the SLN in a rat. For all PA images, a 784 nm wavelength laser was used. (a) Photograph of the rat after the hair was removed from the scanning region before taking the photoacoustic images. The scan region is marked with a black dotted square. (b) Control photoacoustic image without SWNTs injection. Bright parts represent optical absorption, here, blood vessels (BV). (c) After-injection photoacoustic MAP image. The SLN is marked with a red dotted circle. (d) 190 min after-injection photoacoustic MAP image. SLN can also be seen in this image. (e) Photograph of the rat with the skin removed after photoacoustic imaging was done. (f) The excised lymph node. (g) B-scan PA image corresponding to the control image 3(b) (h) B-scan PA image corresponding to the post injection image in figure 3(d). The bright spot represents the PA signal generated from the SLN, marked with red arrow.

Our results show that non-invasive *in vivo* PA imaging for SLN identification with the use of SWNTs as a contrast agent is highly feasible in a small animal model. Moreover, the PA imaging technique used here to image rat SLN can easily be translated to humans. Although, SLN mapping using different contrast agents, e.g., carbon nanotubes, gold nanocages, gold nanorods, and methylene blue dye, has been done successfully, we believe SWNTs have many advantages over the other materials. The broad absorption spectrum of SWNTs will provide us a wide range of light wavelengths for imaging. Most of the other contrast agents have narrow absorption spectra, restricting their use to a particular wavelength. SWNTs also show good efficacy as contrast agents for thermoacoustic imaging.[21] In the future, thermoacoustic tomography can also be combined with PA imaging system for SLN mapping. Targeted SWNTs could also be used for more specific identification. Currently, this imaging system is limited by its slow scanning speed. Employing a higher pulse-repetition-frequency laser and an ultrasound array system could accelerate acquisition, potentially allowing real-time PA imaging. The *in vivo* biocompatibility of SWNTs needs to be thoroughly examined before its translation for clinical use. Nevertheless, since SLN identification by PA imaging is totally non-invasive and safe, it shows potential future clinical applications without the limitations of current invasive and minimally-invasive techniques.

4. SUMMARY

We were able to indentify SLN non-invasively using SWNTs as a contrast agent. In the future, targeted SWNTs could be used for more specific identification. The broad photoacoustic spectrum of SWNTs will provide us wide choices of light wavelength for imaging. Currently, this imaging system is limited by its slow scanning speed. Employing a higher pulse-repetition-frequency laser, say, 50 Hz, and an ultrasound array system could accelerate acquisition, potentially allowing real-time PA imaging. Since photoacoustic SLN identification using SWNTs is totally non-invasive and safe, it has potential future applications in the identification of SLNs *in vivo* in clinical practice, thus reducing the patient's morbidity.

5. ACKNOWLEDGEMENTS

This work was supported by National Institutes of Health grants (R01 EB000712, R01 NS46214 (Bioengineering Research Partnerships), R01 EB008085, and U54 CA136398 (Network for Translational Research) - LVW) and the Office of the Vice President of Research at Stony Brook University, Carol M. Baldwin fund (SB). L.W. has a financial interest in Endra, Inc., which, however, did not support this work. The authors would like to thank Dr. Oleg Gang and Dr. Huming Xiong at the Center for Functional Nanomaterials, Brookhaven National Laboratory for access to the AFM, Mr. Tom Salagaj and Mr. Christopher Jensen at FirstNano/CVD Equipment Corporation for access to their CVD facilities and Dr. Eunah Lee at Horiba JvonYvon, Edison, NJ for the Raman Spectroscopy measurements.

REFERENCES

[1] Early stage breast cancer, Consens Statement, 8:1 (1990).

[2] Swenson, K. K., Nissen, M. J., Ceronsky, C., Swenson, L., Lee, M. W., and Tuttle, T. M., "Comparison of side effects between sentinel lymph node and axillary lymph node dissection for breast cancer," Annals of Surgical Oncology, 9, 745-753 (2002).

[3] Krag, D., Weaver, D., Ashikaga, T., Moffat, F., Klimberg, V. S., Shriver, C., Feldman, S., Kusminsky, R., Gadd, M., Kuhn, J., Harlow, S., and Beitsch, P., "The sentinel node in breast cancer - A multicenter validation study," New England Journal of Medicine, 339, 941-946 (1998).

[4] McMasters, K. M., Tuttle, T. M., Carlson, D. J., Brown, C. M., Noyes, R. D., Glaser, R. L., Vennekotter, D. J., Turk, P. S., Tate, P. S., Sardi, A., Cerrito, P. B., and Edwards, M. J., "Sentinel lymph node biopsy for breast cancer: A suitable alternative to routine axillary dissection in multi-institutional practice when optimal technique is used," Journal of Clinical Oncology, 18, 2560-2566 (2000).

[5] Ung, O. A., "Australasian experience and trials in sentinel lymph node biopsy: the RACS SNAC trial," Asian J. Surg., 27, 284-290 (2004).

[6] Purushotham, A. D., Upponi, S., Klevesath, M. B., Bobrow, L., Millar, K., Myles, J. P., and Duffy, S. W., "Morbidity after sentinel lymph node biopsy in primary breast cancer: Results from a randomized controlled trial," Journal of Clinical Oncology, 23, 4312-4321 (2005).

[7] Brancato, B., Zappa, M., Bricolo, D., Catarzi, S., Risso, G., Bonardi, R., Cariaggi, P., Bianchin, A., Bricolo, P., Rosselli Del Turco, M., Cataliotti, L., Bianchi, S., and Ciatto, S., "Role of ultrasound-guided fine needle cytology of axillary lymph nodes in breast carcinoma staging," Radiol. Med. (Torino), 108, 345-355 (2004).

[8] Deurloo, E. E., Tanis, P. J., Gilhuijs, K. G. A., Muller, S. H., Kroger, R., Peterse, J. L., Rutgers, E. J. T., Olmos, R. V., and Kool, L. J. S., "Reduction in the number of sentinel lymph node procedures by preoperative ultrasonography of the axilla in breast cancer," European Journal of Cancer, 39, 1068-1073 (2003).

[9] Krishnamurthy, S., Sneige, N., Bedi, D. G., Edieken, B. S., Fornage, B. D., Kuerer, H. M., Singletary, S. E., and Hunt, K. K., "Role of ultrasound-guided fine-needle aspiration of indeterminate and suspicious axillary lymph nodes in the initial staging of breast carcinoma," Cancer, 95, 982-988 (2002).

[10] Patel, C. K. N., and Tam, A. C., "Pulsed optoacoustic spectroscopy of condensed matter," Rev. Mod. Phys., 53, 517 (1981).

[11] Hoelen, C. G. A., de Mul, F. F. M., Pongers, R., and Dekker, A., "Three-dimensional photoacoustic imaging of blood vessels in tissue," Optics Letters, 23, 648-650 (1998).
[12] Wang, X. D., Pang, Y. J., Ku, G., Xie, X. Y., Stoica, G., and Wang, L. H. V., "Noninvasive laser-induced photoacoustic tomography for structural and functional in vivo imaging of the brain," Nature Biotechnology, 21, 803-806 (2003).
[13] Song, K. H. and Wang, L. H. V., "Deep reflection-mode photoacoustic imaging of biological tissue," Journal of Biomedical Optics, 12, 060503 (2007).
[14] Laser Institute of America, American National Standard for Safe Use of Lasers ANSI Z136.1-2000 (American National Standards Institute, Inc., New York, NY, 2000).
[15] Marquez, G., Wang, L. H. V., Lin, S. P., Schwartz, J. A., and Thomsen, S. L., "Anisotropy in the absorption and scattering spectra of chicken breast tissue," Applied Optics, 37, 798-804 (1998).
[16] Tromberg, B. J., Coquoz, O., Fishkin, J., Pham, T., Anderson, E. R., Butler, J., Cahn, M., Gross, J. D., Venugopalan, V., and Pham, D., "Non-invasive measurements of breast tissue optical properties using frequency-domain photon migration," Philosophical Transactions of the Royal Society of London Series B-Biological Sciences, 352, 661-668 (1997).
[17] Fu, Q., Huang, S. M., and Liu, J., "Chemical vapor depositions of single-walled carbon nanotubes catalyzed by uniform Fe2O3 nanoclusters synthesized using diblock copolymer micelles," Journal of Physical Chemistry B, 108, 6124-6129 (2004).
[18] Zhang, H. F., Maslov, K., Stoica, G., and Wang, L. H. V., "Functional photoacoustic microscopy for high-resolution and noninvasive in vivo imaging," Nature Biotechnology, 24, 848-851 (2006).
[19] Margenthaler, J. A., "Depth measurement of sentinel lymph nodes in human," Unpublished data (2007).
[20] De La Zerda, A., Zavaleta, C., Keren, S., Vaithilingam, S., Bodapati, S., Liu, Z., Levi, J., Smith, B. R., Ma, T. J., Oralkan, O., Cheng, Z., Chen, X. Y., Dai, H. J., Khuri-Yakub, B. T., and Gambhir, S. S., "Carbon nanotubes as photoacoustic molecular imaging agents in living mice," Nature Nanotechnology, 3, 557-562 (2008).
[21] Pramanik, M., Swierczewska, M., Green, D., Sitharaman, B., and Wang, L. H. V., "Carbon nanotubes as a multimodal – thermoacoustic and photoacoustic – contrast agent," Advanced Materials 2009 (Under Review).